Quaternary Science Reviews 131 (2016) 179–192

Contents lists available at ScienceDirect

Quaternary Science Reviews

journal homepage: www.elsevier.com/locate/quascirev

Geochemical and geomorphological evidence for the provenance of aeolian deposits in the Badain Jaran Desert, northwestern China

Fangen Hu [a, b], Xiaoping Yang [a, *]

[a] Key Laboratory of Cenozoic Geology and Environment, Institute of Geology and Geophysics, Chinese Academy of Sciences, P.O. Box 9825, Beijing 100029, China
[b] University of Chinese Academy of Sciences, Beijing 100049, China

ARTICLE INFO

Article history:
Received 2 August 2015
Received in revised form
23 October 2015
Accepted 26 October 2015
Available online xxx

Keywords:
Surface process
Desert
Geochemistry
Trace and rare earth elements
Sediment source
Tibetan Plateau
Mongolia
China

ABSTRACT

Identifying provenance of aeolian deposits in the mid-latitude deserts of Asia is essential for understanding formation and changes of Earth surface processes due to palaeoclimatic fluctuations. While some earlier studies focused on the interpretation of palaeoenvironments on the basis of aeolian deposits mainly in the desert margins and inter-dune lacustrine sediments, research on provenance of desert sands in the vast Asian mid-latitude deserts is still rare. In this paper, we present new geochemical data which provide insight to the provenance of dune sands in the Badain Jaran Desert, northwestern China, an important part of this desert belt. We sampled aeolian and lacustrine sediments in various parts of the Badain Jaran Desert, and examined their major, trace and rare earth elements (REE) in bulk samples, coarse and fine fractions, respectively. In addition, we took and analyzed samples from a rarely known dune field with red sands, northeast of the Badain Jaran. Our results show that the sands from the Badain Jaran Desert are generally different from those in the red sand dune field in terms of REE pattern and geochemical characteristics, suggesting different sediment origins. Geochemical composition of the aeolian sand samples indicates these sediments should be mainly derived from mixed source rocks of granite, granitoids and granodiorite. Comparing the immobile trace elements and REE ratios of the samples from the Badain Jaran Desert, red sand dune field with rocks of granite, granitoids in their potential source areas, we conclude that: (1) The aeolian deposits in the Badain Jaran Desert are predominantly derived from the Qilian Mountains, northeastern Tibetan Plateau initially via fluvial processes; (2) The Altay Mountains and Mongolian Gobi are the ultimate source areas for the red sand dune field; (3) The Altai Mountains and Mongolian Gobi in the northwest, that could produce massive amounts of materials via intensive deflation and alluvial process, are additional sand sources of the Badain Jaran Desert although their contribution is of secondary significance. As the Badain Jaran Desert acts as sediment sinks of sediments from the Qilian Mountains of northeastern Tibetan Plateau via fluvial processes, it is likely that zircon grains of loess on the Chinese Loess Plateau with age distributions similar to those of the northern Tibetan Plateau could be derived from the Badain Jaran Desert, as the wind data suggest.

1. Introduction

Aeolian deposits, especially in arid and semiarid desert regions, are significant component of the Earth's surface sediment systems (Thomas and Wiggs, 2008). That provides a large proportion of global dust production. Dust has significant impact on the Earth system referring to radiative balance, hydrological and biogeochemical cycles, climate states (Arimoto, 2001; Hara et al., 2006; Maher et al., 2010). Many works have determined the main source regions of dust through satellites, remotely sensed data, numerical modeling and geochemistry tracing (Honda et al., 2004; Yang et al., 2007; Goudie, 2009; Skonieczny et al., 2011; Scheuvens et al., 2013). Sediment provenance of those main source regions of dust (arid and semiarid desert) is actually much less known, though

* Corresponding author.
E-mail address: xpyang@mail.igcas.ac.cn (X. Yang).

http://dx.doi.org/10.1016/j.quascirev.2015.10.039
0277-3791/

that is important for deciphering the response of surface processes to tectonic and climatic changes, and for understanding operation of the Earth system (Molnar, 2004; Che and Li, 2013; Stevens et al., 2013).

As to the field of paleoenvironmental reconstruction in dryland areas which occupy ca. 36% of the land surface of the globe (Williams, 2014), aeolian deposits such as sand dune, are unique geomorphological and palaeoclimatic proxy (Thomas and Burrough, 2012; Yang et al., 2013, 2015; Williams, 2014), especially with the development and application of OSL dating (Munyikwa, 2005; Lancaster, 2008; Singhvi and Porat, 2008; Chase, 2009; Yang et al., 2011). The conventional view interpreted clusters of ages from aeolian sand sequence as indicating periods of extensive dune activity and dry climate (Preusser et al., 2002; Mason et al., 2009). An alternative view is that dune accumulation is likely to record the cessation of periods of more intense aeolian activity, moreover, the non-accumulating dunes actually represent the periods of dune stabilization and humid climate (Chase and Thomas, 2006; Chase, 2009; Chase and Brewer, 2009). Studies revealed that changes in sand supply or source will lead to a direct opposite interpretation of sand accumulation (Williams, 2015), particularly for fluvial-aeolian systems (Cohen et al., 2010). Thus, identifying the sand provenance is of great importance to correctly interpret the palaeoenvironmental indication of sandy sequences.

Compared with deserts in other parts of the world, the mid-latitude deserts of Asia are much more diverse in terms of landscape types and formation processes. For example, active and stable dunes occupy as much as 45% of the deserts of northern China, the eastern portion of the Asian mid-latitude desert belt. In contrast, aeolian sands cover only less than 1% of the arid zone in the Americans (Yang and Goudie, 2007). Among all deserts in China, the Badain Jaran Desert is known particularly for the occurrence of the tallest dunes on Earth (Yang et al., 2011a; Dong et al., 2013). However, the provenance of the sands making the Badain Jaran Desert is still not well understood due to lack of detailed and systematic research. Much earlier effort has been focused on the environmental and climatic changes recorded by the aeolian and lacustrine deposits in the desert and its margins (Yang et al., 2003, 2010, 2011; Gao et al., 2006; Guo et al., 2014; Wang et al., 2015).

Earlier studies assumed that the sandy materials in the Badain Jaran should have been derived from the weathered and denuded products of the underlying Mesozoic and Cenozoic sandstones, sandy conglomerate, clastic rocks (Lou, 1962; Sun and Sun, 1964) and the extensive lacustrine sediments of dry lake beds in the west and northwest (Yang, 1991; Yan et al., 2001), and the giant alluvial fan of Heihe River (Mischke, 2005; Wünnemann et al., 2007). However, these opinions are lack of convincing evidence and have not been verified.

Geochemical fingerprinting has great potential for identifying the provenance of sediments and their transport pathways (Taylor and McLennan, 1985; McLennan, 1989; Muhs et al., 1996, 2003, 2013; Cullers and Podkovyrov, 2002; Ferrat et al., 2011; Lancaster et al., 2015), particularly the trace and rare earth elements (REE), because they are less fractionated during the weathering, transport and sedimentation (Murray, 1994; López et al., 2005; Moreno et al., 2006; Kasper-Zubillaga et al., 2007; Castillo et al., 2008). In this paper, we present our new studies about major and trace elements and REE in the sediment samples collected from various parts of the Badain Jaran Desert and from a small dune field located in its northeast side. In association with the regional geological background and wind data, these geochemical data are further applied to interpret the sources of the Badain Jaran sands which should have an important impact on the Earth's surface system via global dust cycles.

2. Geological and physiogeographical settings

The Badain Jaran Desert lies in the northwest of the Alashan Plateau in the western Inner Mongolia, China, covering an area of 49,000 km^2 (Yang et al., 2011). It is a part of the Alashan Desert region including Tengger and Wulanbuhe deserts, and surrounded by mountain ranges such as Mongolia Altay in the North, Beishan in the northwest and Qilian Mountains in the south (Fig. 1). Mongolia Altay Gobi range, the largest accretionary orogenic collage in the world (Windley et al., 2007), is known in its more extensive equivalent as the Central Asian Orogenic Belt (CAOB). The entire Gobi Corridor region is characterized by a basin and range physiography with discontinuous mountain blocks trending WNW, E-W and ENE. Thick alluvial deposits of late Miocene-Recent age are widespread throughout the region (Cunningham, 2013). Aeolian deflation is a major erosional process throughout the region that provides windblown sediments to the huge Chinese Loess Plateau (CLP) in the southeast direction since at least the late Miocene (Heller and Liu, 1984). The Beishan, situated in the southernmost Altaids (Fig. 1), is a typical accretionary orogenic belt within the Altaids, and topographic culmination is Mazong Mountain. Intrusive rocks occur widely, and are main granitic in composition (Tian et al., 2014). The Qilian Mountains is the foreland region of the Northern Tibetan Plateau (NTP), which is a long-lived accretionary orogen formed in response to the closure of an oceanic basin between the Central Qilian and North China plates in the Paleozoic (Yan et al., 2010). The bedrocks are dominated by Precambrian granitic gneisses with minor Proterozoic granitoids and migmatites (Huang et al., 2014). It crops out overlain by early Paleozoic sedimentary rocks (Harris et al., 1988).

Geologically, the Alashan Plateau is a long-term and stable uplift and denudation area and consists in some faults and basins on the southern part. The Badain Jaran Desert developed in the fault basins and its boundaries are consistent with occurrence of faults. To the north, it is bounded by the Guaizihu wetland, which merges with the Gobi and plains of Mongolia. Jurassic, Cretaceous and Tertiary lacustrine sediment, with thickness of up to 300 m, can be found on the western edge of Badain Jaran Desert (Cai, 1986). Sporadically distributed Yardangs composed of alternations of fine-grained lacustrine and aeolian sand deposits, are exposed in the interdune areas or covered by shifting dunes in Guaizihu and Gurinai (Yang, 1991; Yan et al., 2001).

Climatically, the Badain Jaran Desert, located in the marginal area of East Asian Summer Monsoon, is characterized by a strongly continental climate, with a mean annual temperature of 7.7 °C in the southern portion and 8.2 °C in the northwest (Yang et al., 2010). Mean annual precipitation decreases significantly from ~120 mm in the south to 40 mm in the north of the desert (Yang et al., 2010). The wind strength and direction are mainly controlled by the East Asian Monsoon system, presenting the alternation of southeast winds in summer and northwest winds in winter. Wind rose based on monthly records from 1983 to 2012 displays a distribution pattern dominated by northwest winds (Fig. 1), which is driven by winter monsoon blows from the Siberian High Pressure System.

3. Materials and methods

Eighteen aeolian sand samples (marked by B1-18) and eight lacustrine sediment samples (marked by L1-8) were collected from various parts of the Badain Jaran Desert (Fig. 1). Sample numbers are generally ordered from north to south, with smaller numbers marking the sediments in the north. The aeolian sand samples were collected from the surface of active dunes. Lacustrine sediments are characterized by fine grain size, flat beddings or laminations and clayey and calcareous cementations, while two samples (L1-2)

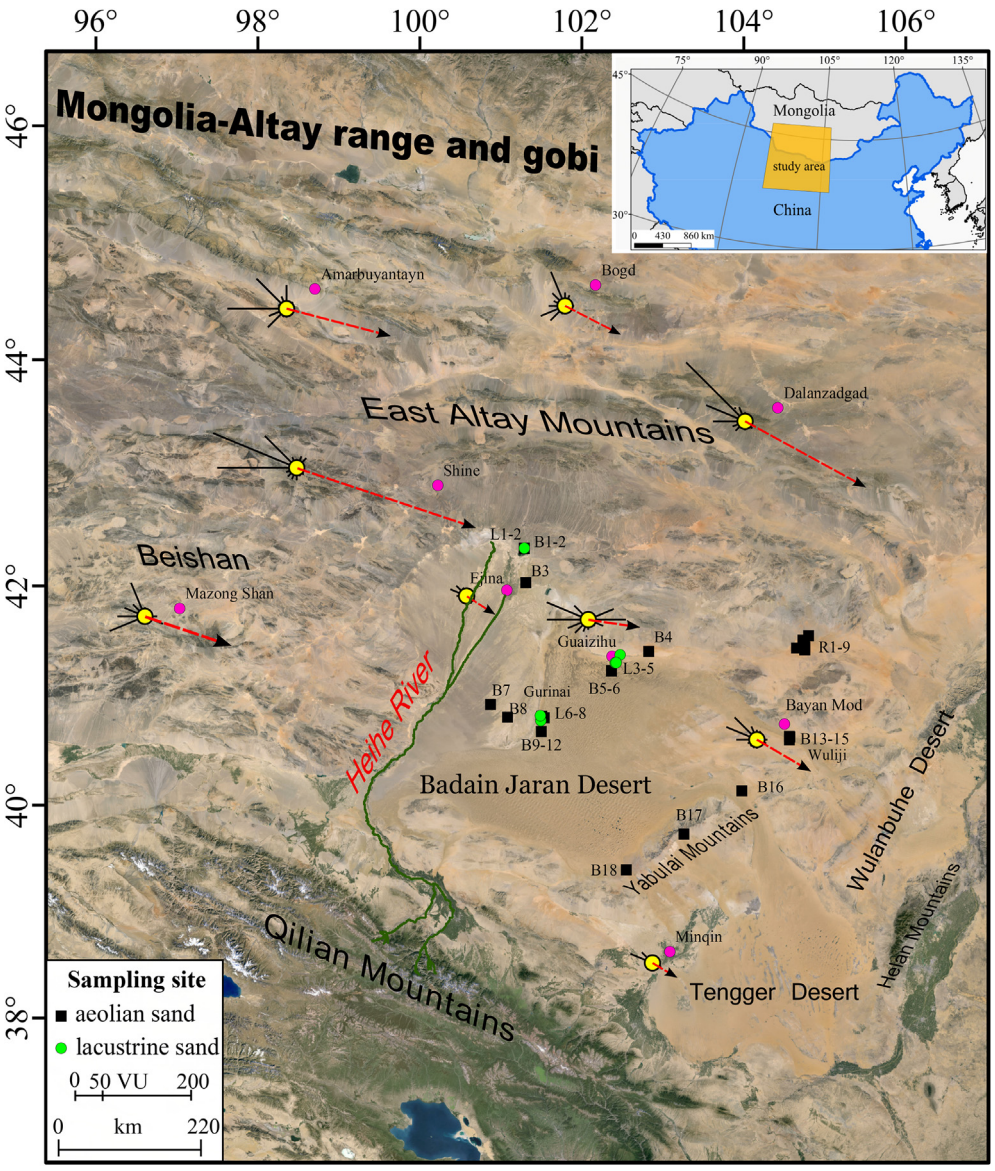

Fig. 1. Location of the study area and sampling sites (image modified from the Google Earth). Sand roses calculated following Fryberger and Dean (1979) with data from the U.S. National Climatic Data Center (NCDC), black lines showing winds capable of transporting sand from various directions (DP) and red arrows indicating the resultant sand transport trends (RDP, Table 1). (For interpretation of the references to colour in this figure legend, the reader is referred to the web version of this article.)

were taken from the middle depth of ca. 10 m high outcrops of old lake sediments, others from exposed surface layers of the dried lake beds. Lacustrine sediments are widely distributed in the northwest Badain Jaran Desert and cover a large age span, from the Holocene to Late Pleistocene (Wünnemann et al., 2007; Yang et al., 2010). For the first time, we investigated a small dune field with only red linear dunes northeast of the Badain Jaran Desert (Fig. S1). This dune field is located on the piedmont of the eastern Altay Mountains. Nine samples (marked by R1-9, numbers are ordered from north to south) were collected from the dune ridges occurring in this red sand dune field (Fig. 1).

Considering different grain size fractions of sediments may have different transport processes and sources, aeolian sand samples were firstly separated into two different grain-size fractions by dry sieving. Samples of B1-18 were isolated to coarse grain size fractions (>250 μm) and fine grain size fractions (<125 μm) (the fraction <63 μm is not sufficient for geochemical analysis). In some samples only one fraction sub-sample (coarse or fine) could be extracted. Due to the generally fine grain sizes in the samples R1-9 only the fine fraction (<63 μm) was extracted (i.e., no coarse fraction available). In addition to the different grain size fractions, geochemical measurement was done on all bulk samples.

Major elements were determined using X-ray Fluorescence Spectrometry (XRF) at the Institute of Geology and Geophysics, Chinese Academy of Sciences. Pretreatment procedures of the samples were as described in Yang et al. (2007a). Analytical uncertainties are ±2% for all major elements except for P_2O_5 and MnO (up to ±10%). Loss on ignition (LOI) was obtained by weighing after 1 h of heating at 950 °C. Chemical index of alteration (CIA) was calculated using a modification of the formula proposed by Nesbitt and Young (1982), i.e. $CIA = [Al_2O_3/(Al_2O_3+CaO^*+Na_2O + K_2O)] \times 100$ (ratio in molecular proportions). Here the CaO^* refers to the amount of CaO only incorporated in the silicates and is calculated after reducing CaO from calcium carbonates. The content of calcium carbonate was determined with a volumetric calcimeter (Eijkelkamp Corp., Netherlands), and the amount of CO_2 was quantified by

adding dilute HCl to the samples in a closed system under constant pressure, temperature and absence of other gases. The error bar for the measurement of the calcium carbonate is less than ±5%.

Trace elements and rare earth elements were determined using an ICP–MS in the Beijing Research Institute of Uranium Geology, Chinese Ministry for Nuclear Industries. Rh was used as the internal standard. The samples were digested in HNO3 (1:1) and HF under high temperature and pressure following a four-step procedure as detailed in Yang et al. (2007a). The analytical uncertainties (relative standard deviation) are less than ±5% and under ±1% for determining REE.

Wind records (data obtained online from the U.S. National Climatic Data Center) covering the period from 1983 to 2012 from the nine meteorological stations at the periphery of the study area were used to interpret the potential movement of sand. Sand drift potential (DP), resultant drift potential (RDP), the directional variability (RDP/DP) and the resultant direction of sand movement (RDD) were calculated (Table 1) following Fryberger and Dean (1979).

4. Results

Original laboratory data of all measurements are listed in Appendix A of supplementary materials. Key features are described below.

4.1. Major elements

Over all, the aeolian sands in the Badain Jaran Desert have a higher SiO_2 and lower other major elements than do samples of red sand dune field. Compared with the Upper Continental Crust (UCC) (Taylor and McLennan, 1985), bulk and coarse fractions of aeolian sands in the Badain Jaran Desert are enriched in SiO_2, while other major elements experience a varying degree of depletion, except for the samples B2 and B9 (Fig. 2). Sample B9 has a high CaO concentration, and a calcareous cementation was also observed in field. Due to preferential enrichment of quartz minerals in the coarse aeolian sands, fine aeolian sands contain a lower percentage of SiO_2, but a higher concentration of Al, Fe, Ca, Mg, K, Na, Ti, Mn than coarse aeolian sands. Enrichment of Ti in fine aeolian sands is very remarkable (Fig. 2), reflecting the existence of Ti-bearing minerals such as ilmenite, rutile and titanite. Lacustrine sands show a greater degree of enriched CaO, with a high calcium carbonate concentration ranging from ~30 to 46%, but all other major elements are depleted, except for the sample L4. L4 shows an enrichment of Fe_2O_3, and a higher concentration of MnO. The UCC-normalized spider diagram of the major elements (Fig. 2) show that aeolian sands in the red sand dune field are rather uniform, while the lacustrine sediments and aeolian sands in Badain Jaran Desert are heterogeneous. Almost all samples, except for L4, show a significant correlation between Fe_2O_3, TiO_2 and MgO (Fig. S2), suggesting the similarity in host minerals between different grain-size fractions and samples. The average CIA of bulk samples, coarse, fine fractions and lacustrine sediments in the Badain Jaran Desert are 54.1, 53.2, 57.1 and 51.8, respectively. The samples from the red sand dune field have a mean CIA of 57.2. K usually resides in K-feldspar mineral, and K-feldspar is more resistant to chemical weathering than plagioclase (Cox et al., 1995). Fig. 3 shows that K is relatively uniform for different fractions in all samples, indicating K less affected by the post-depositional chemical weathering, consistent with the lower CIA values (Appendix A).

Table 1
Sand drift potential (DP), resultant drift potential (RDP), the resultant direction of sand movement (RDD, 0 referring to the north, clockwise) and the directional variability (RDP/DP) based on wind records at the margins of the Badain Jaran Desert from 1983 to 2012 (vector units with wind speed in knots).

Station	Latitude	Longitude	DP	RDP	RDD	RDP/DP
Amarbuyantayn	44.62°	98.7°	472	340	105	0.72
Bayan Mod	40.75°	104.5°	281	194	120	0.69
Bogd	44.65°	102.17°	323	195	117	0.6
Dalanzadgad	43.58°	104.42°	527	437	119	0.83
Ejina	41.95°	101.07°	75	58	123	0.78
Guaizihu	41.37°	102.37°	578	138	98	0.24
Mazong Shan	41.8°	97.03°	396	215	110	0.54
Minqin	38.63°	103.08°	89	72	120	0.8
Shine	42.9°	100.22°	743	599	107	0.81

4.2. Trace elements

The UCC-normalized abundances of selected trace elements for the different samples and grain size fractions are shown in Fig. 3. Most trace elements, except for Sb, show a greater degree of depletion for bulk and coarse fraction sands in the Badain Jaran Desert. However, for the fine fraction, enrichments of Cr, Ni, Zr, Hf, Cd, Sb, and Bi are very obvious, and almost all trace element concentrations in fine fractions are higher than those in the coarse fractions. Compared with the aeolian sands in the Badain Jaran Desert, lacustrine sediments show a large variation range, and have a higher U, Rb, Ba contents arising from the impact of carbonate, but a similar enrichment of Cd and Sb to that in the fine fraction of aeolian sands. Most of the selected trace elements are enriched in the sands of the red sand dune field, particularly the high field-strength elements (HFSE) Zr and Hf, which are nearly 2 to 7 times of those of UCC. Most of the selected trace elements' concentrations in the sands in the red sand dune field are higher than those in the Badain Jaran Desert sands. However, the contents of Cr and Ni in the Badain Jaran Desert, possibly related to the ophiolite of bulk and fine fractions, are higher than those in red sand dune field.

4.3. Rare earth elements

In the Badain Jaran Desert, the mean total REE contents are 57.7 ppm in the bulk dune sand samples, 40.2 ppm in their coarse fractions, 111.9 ppm in their fine fractions, and 49.9 ppm in lacustrine sediments, respectively (for more details see Appendix A). In contrast, samples from red sand dune field have a much higher REE concentration with an average of 116.1 ppm in bulk samples and 242.2 ppm in fine fractions. Although the REE abundances are greatly different, the chondrite-normalized REE distribution patterns of both samples from the Badain Jaran Desert and the red sand dune field are characterized by steep light-REE (LREE) and relatively flat heavy-REE (HREE) shapes and with negative Eu anomalies (Fig. 4). These REE distribution features are broadly identical to those of UCC (Taylor and McLennan, 1985), especially for the fine fractions of the sands in the Badain Jaran Desert and bulk samples from the red sand dune field. The higher REE contents in the fine fractions are probably due to lower content of quartz, consistent with the concentration of major elements (Fig. 2). The coarse fraction of sand sample B13 and lacustrine sample L3 have the lowest REE content among all sample (20.1 ppm and 23.2 ppm, respectively), while they have the highest SiO_2 content (86%) and calcium carbonate (46%), respectively.

Although the shapes of REE patterns are similar, the aeolian sand and lacustrine sediments differ in Ce and Eu anomalies and La_N/Yb_N and Gd_N/Yb_N ratios (Fig. 5). Fine fractions of the samples from the Badain Jaran Desert and the samples from the red sand dune field with slight negative Ce anomalies are with Ce/Ce* and La_N/Yb_N ratios generally greater than 0.95 and 7, respectively. Fine fraction sands show the most severe negative Eu anomalies, with

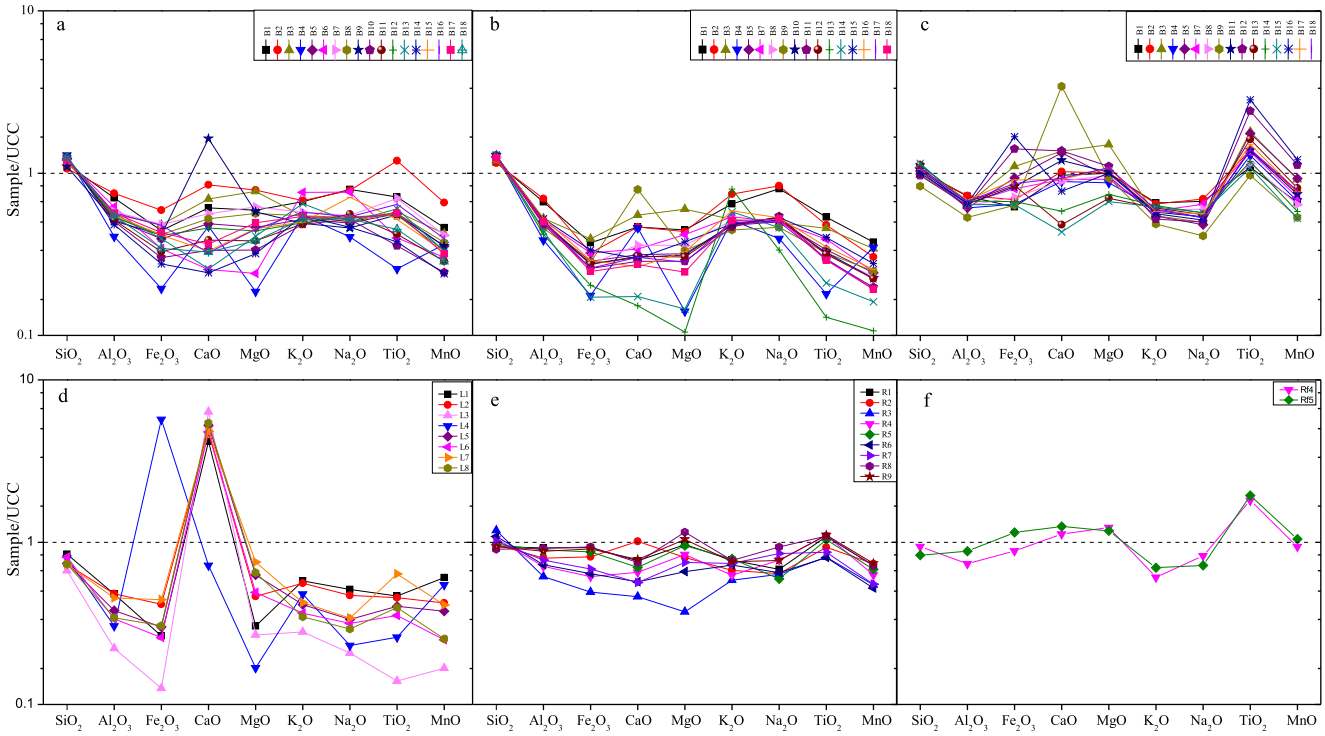

Fig. 2. UCC-normalized spider diagrams of major elements. (a), (b), (c) are for bulk, coarse and fine fraction dune sands in the Badain Jaran Desert, respectively; (d) is for lacustrine sediments in the Badain Jaran Desert; (e), (f) are for bulk and fine fraction sands in the red sand dune field, respectively.

an average value of 0.59, their Gd_N/Yb_N ratios often greater than 1.2 (Fig. 5), but they are mostly <1.2 in coarse fraction and bulk samples. The Gd_N/Yb_N ratios of most samples from the red sand dune field are larger than 1.2 too.

5. Discussion

5.1. Types of main source rocks of the aeolian sediments

Among all major elements, Ti and Al are the most immobile and insoluble ones, and have the lowest solubility in natural water. Al_2O_3/TiO_2 ratio is thus an effective indictor in tracing source rock types. According to Girty et al. (1996) and Ahmad and Chandra (2013), an Al_2O_3/TiO_2 ratio <10 in sediments is suggestive of mafic source rocks, whereas ratios in the range >20 are indicators likely to be derived from felsic source rocks, and ratios between 10 and 20 are considered as intermediate source rocks. Only in the fine fraction of sample B15, the TiO_2/Al_2O_3 ratio is < 10 (7), suggesting a mafic source rock. Moderate values of Al_2O_3/TiO_2 ratios in fine fractions of aeolian sands should be therefore attributed to the intermediate source rocks origins. Coarse fraction and bulk samples yields a high Al_2O_3/TiO_2 ratio (>20), demonstrating a felsic source. Lower CIA and Th/U values of all samples (Appendix A) indicate that the aeolian sands both in the Badain Jaran Desert and in the red sand dune field have undergone a low degree of chemical weathering (CIA<60, Th/U < 4). The difference of chemical composition between various grain size fractions should be related to sediment sorting and recycling, because ultra-resistant heavy minerals may preferentially concentrate in fine-grained through multiple recycling of transport and weathering (Castillo et al., 2008; Ferrat et al., 2011).

The trace elements ratios indicate that the aeolian dune sediments have experienced multiple sedimentary cycles, rather than direct from any source rocks. The Zr/Co vs. Th/Co plots have been used to differentiate between mafic and felsic source rocks (McLennan et al., 1993). Our samples, except for the lacustrine sample L4, are much closer to the line of the felsic rocks (Fig. 6), showing the source rock should be mainly felsic. Since Th is typically an incompatible element and Co is typically compatible in igneous rocks, Th/Co ratio is an overall indicator of igneous chemical differentiation processes (Taylor and McLennan, 1985). But, zircon addition resulting from sediment recycling and sorting can lead to Th/Co and Zr/Co ratios not to follow the normal igneous differentiation trend (McLennan et al., 1993). Fig. 6a shows that most data plotted in field between the trend 1 and trend 2, and fine fractions of aeolian sands both in the Badain Jaran and the red sand dune field clustered close to the trend 2, confirming zircon additions rather than pure compositional change trend (trend 1), suggesting strong sedimentary recycling. Ternary diagram of Al–Ti–Zr could reduce the effects of weathering of the absolute contents of Al, Ti, and Zr and highlights the effects of recycling processes of the sediments (Garcia et al., 1994). Fig. 6b demonstrates that the fine fractions of the Badian Jaran sands and those from the red sand dune field are towards the Zr apex, suggesting that strong sedimentary recycling leads to the increase in zircon.

The elements Zr and Hf are generally enriched in zircon, which is virtually ubiquitous in all felsic igneous rocks and is one of the quite stable minerals often resilient to chemical and mechanical destruction. Zr and Hf are very similar crustal incompatible elements and hence can be used to differentiate between different crustal processes. The good correlation between Zr and Hf (Fig. S3) for all samples suggest that they mainly origin from zircons. In addition, the values of Zr/Hf ratio for all samples and fractions lie close to ratio of 40 (Fig. S3), providing evidence of similar crustal rock origin of zircon and further strongly indicating that a granitoid source of the zircon grains (Batchelor and Bowden, 1985) in the red sand dune field and in the Badain Jaran Desert.

The molar ratios of Al_2O_3–(CaO^* + Na_2O)–K_2O plotted in

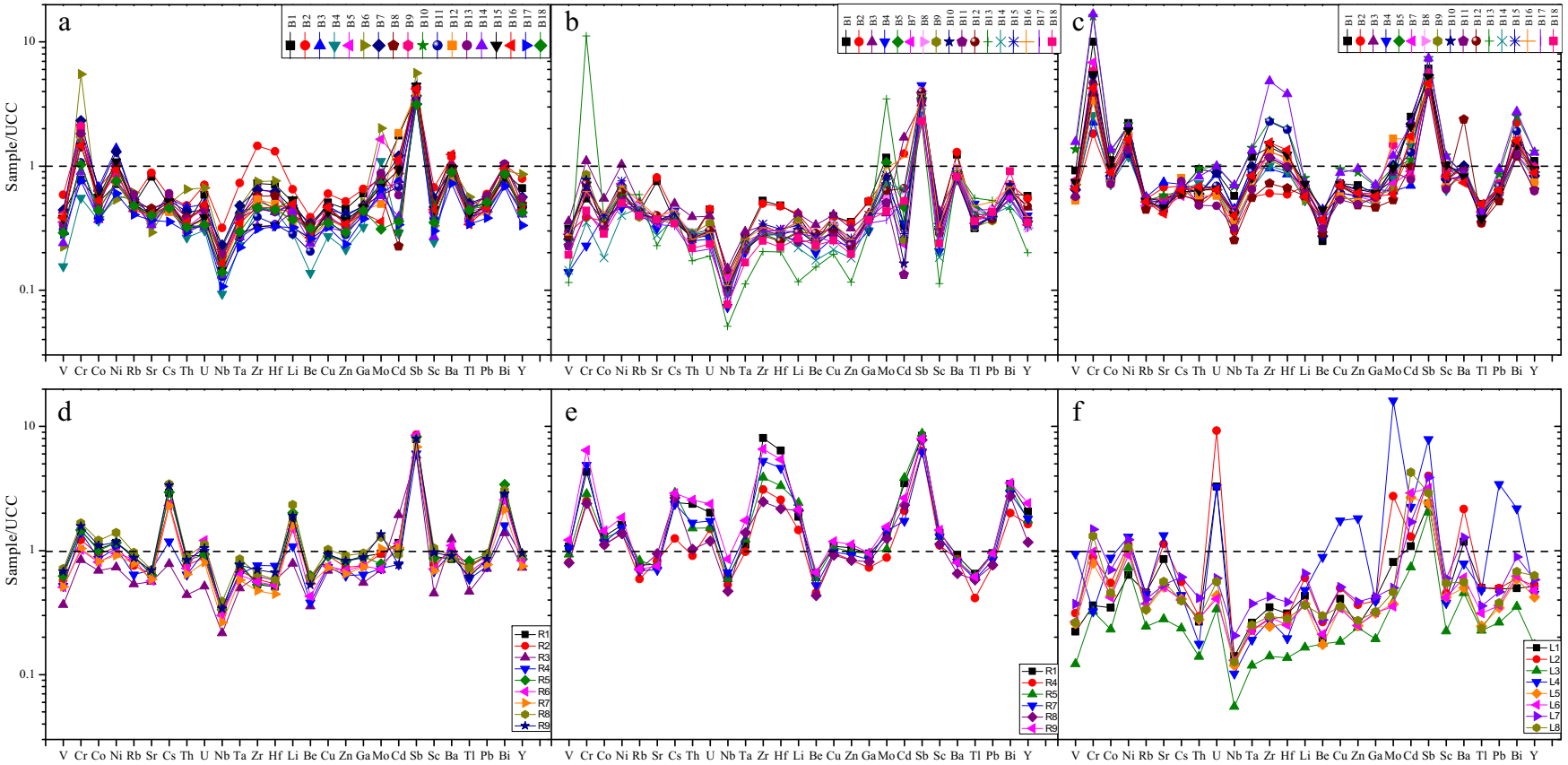

Fig. 3. UCC-normalized trace element patterns for different samples and fractions. (a), (b), (c) are for bulk, coarse and fine fraction dune sands in the Badain Jaran Desert, respectively; (d) and (e) are for bulk and fine fraction sands in the red sand dune field; (f) is for the lacustrine sediments in the Badain Jaran Desert.

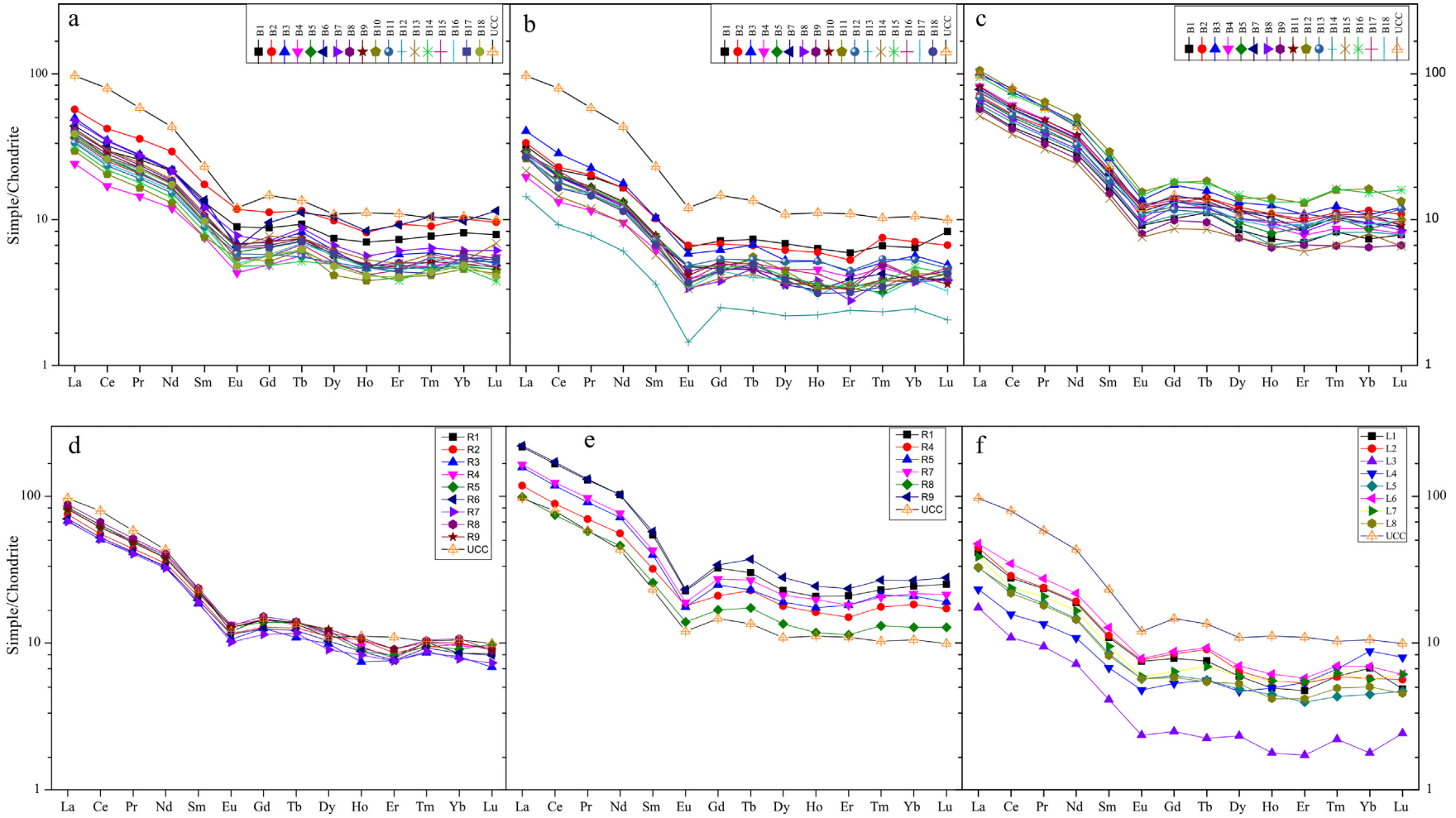

Fig. 4. Chondrite-normalized REE patterns for different sediments and fractions. (a), (b) and (c) are for bulk, coarse and fine fraction dune sands in the Badain Jaran Desert, respectively; (d) and (e) are for bulk and fine fraction sands in the red sand dune field; (f) is for lacustrine sediments in the Badain Jaran Desert.

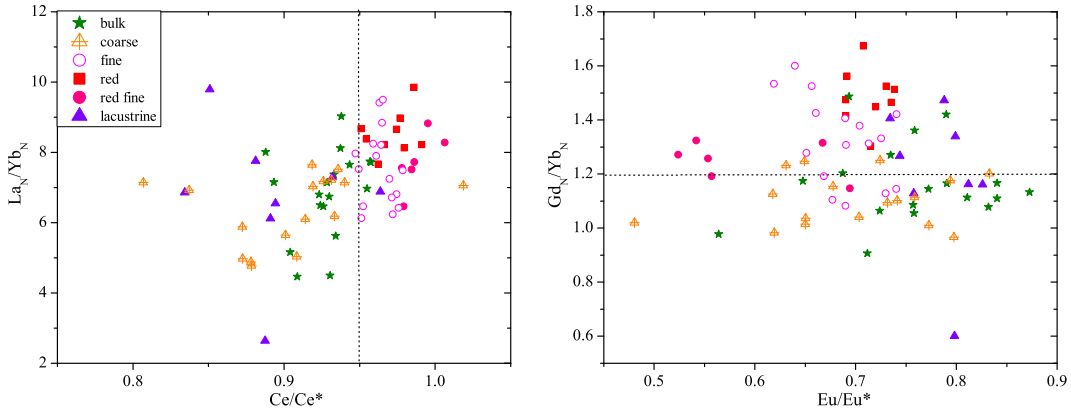

Fig. 5. Plots of Ce/Ce* vs. La_N/Yb_N and Eu/Eu* vs. Gd_N/Yb_N for different sediments and fractions. bulk – Bulk samples of the dune sands from the Badain Jaran Desert; coarse – Coarse fraction of the Badain Jaran dune sands; fine – Fine fraction of the Badain Jaran dune sands; red – Bulk samples from the red sand dune field; red fine – Fine fraction of the sands from the red sand dune field; lacustrine – Lacustrine sediments in the Badain Jaran Desert. (For interpretation of the references to colour in this figure legend, the reader is referred to the web version of this article.)

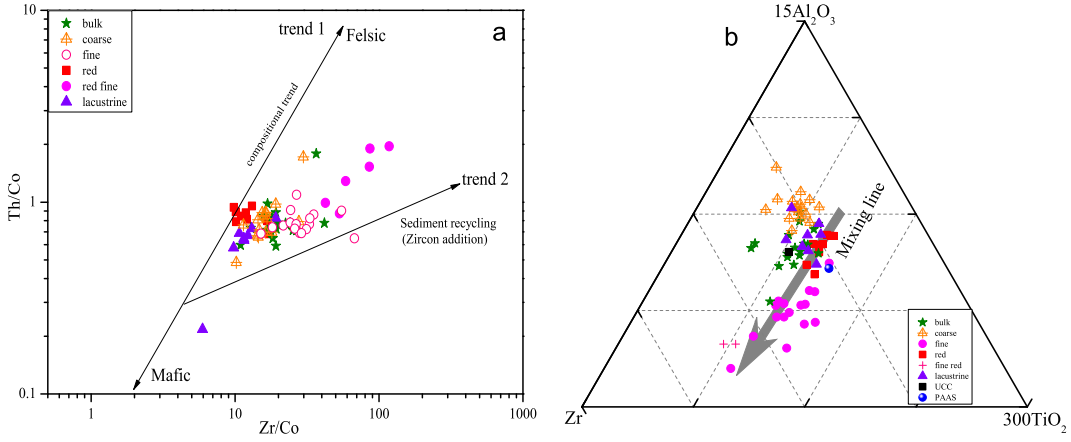

Fig. 6. Plots of Zr/Co vs. Th/Co (a) and Al–Zr–Ti diagram (b) for different sediments and fractions. Keys same as for Fig. 5. UCC = Upper Continental Crust; PAAS = Post-Archean Australian Shale.

triangular A–CN–K diagram reflect the weathering trend and source rock composition of sediments (Fedo et al., 1995; Nesbitt and Markovics, 1997). Before plotting such a molar ratios plot, CaO included in the carbonate minerals and apatite should be subtracted from the total CaO. Here we subtracted the CaO in carbonate minerals based on calcium carbonate content. CaO in phosphates has not been considered in the calculation, because CIA values increase only by ca. 1 unit if all P_2O_5 is assigned to apatite (Bahlburg and Dobrzinski, 2011). On the occasion without K metasomatism, weathering trend line, parallel to A-CN join in the A–CN–K triangle, intersects the feldspar join (Pl-Ks) at the point that reflects the proportion of plagioclase and K-feldspar of the source rocks. This proportion indicates the type and composition of parent rocks (Taylor and McLennan, 1985; Fedo et al., 1995). The A–CN–K diagram (Fig. 7a) shows that weathering trend of our data is parallel to A-CN join, and does not exhibit any inclination towards the K apex, indicating these sediments have not been subjected to any potash metasomatism. The intersection of weathering trend line and the feldspar join (Pl-Ks) (Fig. 7a) lies between the point of granite (G) and granodiorite (Gd), suggesting main source rocks of most samples are probably the granite and granodiorite. However, due to regional geological setting, local variations do exist. For instance, the source rocks for the coarse fraction of sample B14 are probably the A-type granite. Regional geological setting confirms that A-type granite is widely distributed near the site of B14 (Zhang et al., 2013b).

The La and Th shows a good linear relationship for all samples and their different grain size fractions (Fig. S3), and most lie close to the line of La/Th = 3.2, indicating that there are close geochemical associations in these sediments. Th is well correlated to La, Ce and Pr with correlation coefficients (r) > 0.98 and less correlated to Al and Rb in association with clays, suggesting Th is controlled by heavy minerals such as monazite and epidote. Precise data about the concentration of heavy minerals in the aeolian sands in the Badain Jaran Desert are still not available. Yang (1991) studied the concentration of heavy minerals in the grain size fraction 0.01–0.25 mm in the Badain Jaran Desert and found that epidote is one of the commonest heavy minerals and monazite occurs but with a much lower concentration. In this grain size fraction, the total heavy minerals account for less than 3% by weight (Yang, 1991). Thus, it seems clear that Th is mainly controlled by epidote in the sands of the Badain Jaran due to very low abundance of monazite. The La–Th–Sc diagram is often used to discriminate provenance of sediments (McLennan et al., 1993; Cullers and Podkovyrov, 2002). Data of our samples all plot in the field of silicic rock, and fall between the field of granite, granitoids and granodiorite compositions (Fig. 7b), also indicating that sediments are probably derived from mixed source rocks of granite, granitoids

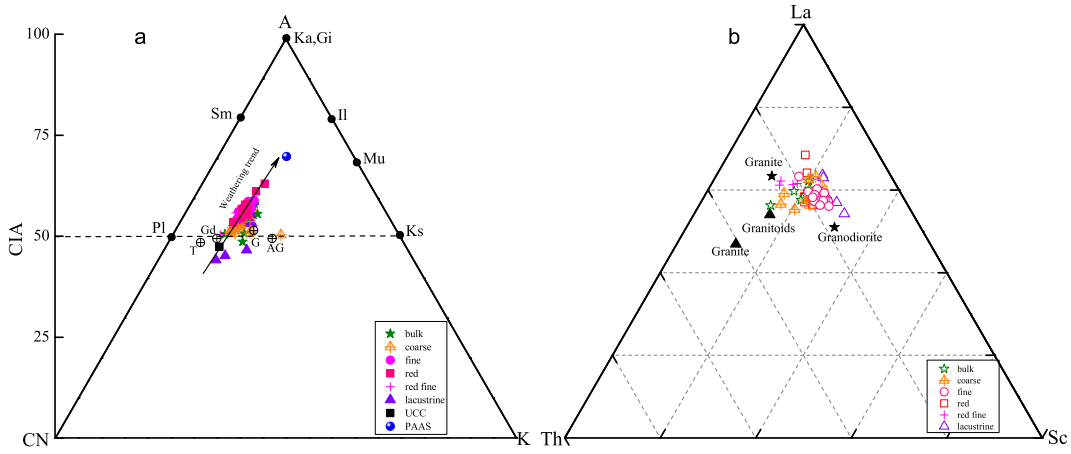

Fig. 7. A–CN–K diagram and CIA (a) and Th–La–Sc diagram (b) for different sediments and fractions. In (a), T = tonalite, Gd = granitoid, G = granite, AG = A-type granite (Taylor and McLennan, 1985; Fedo et al., 1995). In (b), the data of granite and granitoid in solid black triangle and star are from Qilian Mountains (Wan et al., 2006; Yan et al., 2010; Huang et al., 2014) and Altay Mountains and Mongolia Gobi (Economos et al., 2008; Hanzl et al., 2008; Zhang et al., 2013), respectively (Data of the potential source rocks are the average values of several samples with large spatial coverage.). Keys same as for Fig. 6.

and granodiorite.

5.2. Provenances of aeolian sands

As discussed above, geochemical compositions indicate that sediments in the Badain Jaran Desert and in the red sand dune field are mainly derived from granite, granitoids and granodiorite. Even though, granite, granitoids and granodiorite from various geological settings may have different geochemical characteristics probably in response to differing thermal regimes (Taylor and McLennan, 1985; McLennan et al., 1993). Just as shown in the La–Th–Sc diagram (Fig. 7b), the two granite and granitoids data point from the Qilian Mountains and Mongolia-Altay fall in different fields. Thus we can further determine the sediment provenances through the geochemical comparison between the sediments and its potential source rocks.

Our comparison of trace elements and REE ratios of sediments in the Badain Jaran Desert, the red sand dune field with granite, granitoids in their potential source areas of Qilian Mountains and East Altay Mountains and Mongolian Gobi belt reveals more or less overlapping between the two potential source areas (Fig. 8). Most samples from the Badain Jaran Desert fall in or close to field of its potential source area (Fig. 8), indicating Qilian Mountains is an important ultimate source area for the sediments in the Badain Jaran Desert. However, the sediment contribution from the Altay Mountains and Mongolian Gobi cannot be excluded, particularly for those samples falling in the overlapping field and Altay and Gobi area (Fig. 8). Almost all samples from the red sand dune field fall in the potential source areas (Fig. 8b,c,d) or nearby (Fig. 8a), suggesting that the Altay Mountains and Mongolian Gobi are the ultimate source areas for the red sand dune field. Our field investigation confirms that the aeolian sediments in this small separate dune field should be from fluvial and alluvial deposits from the north.

Fig. 9 shows the variations of some trace elements and REE ratios, which should be independent of particle size variations (Ferrat et al., 2011), confirming difference between the Badain Jaran Desert and the red sand dune field. Data of the red sand dune field in the Nb versus Y (Fig. S3) plot are off the linear array formed by the data of Badain Jaran Desert, and the data of the red sand dune field show a better correlation between Nb and Y, also meaning that the minerals controlling Y contents are different between these two dune fields.

The lacustrine sands fall in same field as the aeolian sands in the Badain Jaran Desert (Fig. 9), confirming that the extensive lacustrine sediments of the currently dry lake beds in the west and northwest could be important sand sources for the Badain Jaran Desert (Yang, 1991; Yan et al., 2001), as indicated by the negative Ce anomalies. Negative Ce anomalies are well known in the sediments of marine, river, lake and marsh environments (Condie et al., 1995). For deserts or aeolian systems in general, the adjacent exposed areas of lake beds and river channels are significant sand sources for dune development (Williams, 2014; Lancaster et al., 2015).

The Heihe River mainly drains the north flank of the Qilian Mountains, and carries about 40,000 tons of sediments per year to the giant alluvial–proluvial fan in the lower reaches at present (Yan et al., 2001). It carries not only the sediments eroded from the Qilian Mountains, but also sediments washed from the Beishan (mountains) by some ephemeral streams, and the silty sands blown from Mongolia (Li et al., 2011; Che and Li, 2013). Dense ephemeral channels originating from the east Altay Mountains (Fig. S4) demonstrate that large amount of sediments would be transported from the Mongolian Altay to the Ejina basin. Even more, during the local wet periods of MIS 3 and mid-Holocene (Yang et al., 2010, 2011), strong fluvial input from the Altay Mountain ranges would be inevitable (Wünnemann et al., 2007). Thus the Ejina basin acts as a sediment sink not only for the Qilian Mountains but also for the Altay Mountains. Since the Altay Mountains and Mongolian Gobi are located in the predominately upwind direction of the Badain Jaran Desert and in a high-energy wind environment indicated by DP value > 400 VU (Fig. 1, Table 1), sediment contribution from Altay Mountains and Mongolian Gobi could be reasonably large, consistent with the indication of our geochemical data (Fig. 9).

Sediment sources and their transport pathways for the Badain Jaran Desert are schematically shown in Fig. 10. In terms of quantitative contribution, Altay Mountains and Mongolian Gobi should be much smaller than the Qilian Mountains, as indicated by geochemical tracing. I.e., only a small number of samples from the Badain Jaran Desert fall in the same field with the red sand dune field in plots of La_N/Yb_N vs. Zr/Hf, La_N/Yb_N vs. Nb/Ta, Gd_N/Yb_N vs. La/Th, La_N/Gd_N vs. Gd_N/Er_N (Fig. 9). This is mainly due to different geomorphological and hydrological factors. The high relief and frequent and intense glacier activities in the Qilian Mountains can yield much more loose materials than east Altay Mountains (Jolivet et al., 2007). Secondly, runoff volume of the Heihe River drainage is much greater than the ephemeral channels or past perennial

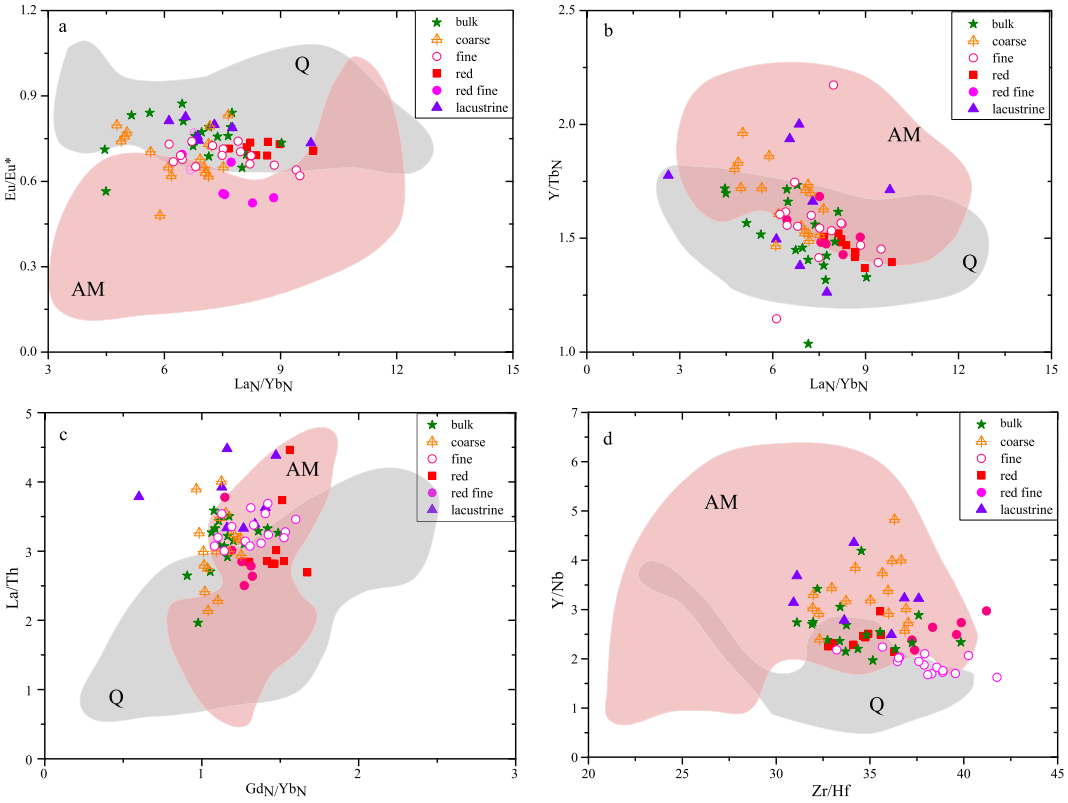

Fig. 8. Bivariate diagrams of trace and rare earth element ratios of sample from the Badain Jaran Desert and the red sand dune field, and compared to their potential source areas. AM field is potential source areas of Altay Mountains and Mongolia Gobi (data from Economos et al., 2008; Hanzl et al., 2008; Zhang et al., 2013); Q field is potential source areas of Qilian Mountains (data from Wan et al., 2006; Yan et al., 2010; Huang et al., 2014). Keys same as for Fig. 6.

channels with headwaters in the eastern Altay Mountains and Beishan (Fig. 10).

Our interpretation of the sediment sources for the Badain Jaran Desert is supported by studies of detrital zircons in the region. U–Pb ages and shape of detrital zircons, sediment Nd–Sr isotopic tracer and ESR signal intensity of quartz also demonstrated a relatively small sediment contribution from Altay Mountains and Mongolian Gobi to Alashan drylands (Sun et al., 2007; Li et al., 2011; Che and Li, 2013; Zhang et al., 2013a). For example, the latest published U–Pb ages of detrital zircon from alluvial–proluvial fans of the Heihe River revealed that contribution of sediments from the Altay Mountains and Mongolian Gobi could explain the higher age probability at ~360 Ma, which exactly matched with zircon age of Altay Mountains and Mongolian Gobi (Che and Li, 2013). Li et al. (2011) suggested that two end members of lower ε_{Nd} value, higher $^{87}Sr/^{86}Sr$ ratio and higher ε_{Nd} value, lower $^{87}Sr/^{86}Sr$ ratio in south and north Alashan drylands should point to different sources (Fig. 11). A similar distribution also appears in our data plot of Y/Ni vs. Cr/V (Fig. 11), that is often used to evaluate relative proportion of ultramafic and felsic rocks in the source regions (McLennan et al., 1993; Amorosi et al., 2002).

Mafic-ultramafic rocks such as ophiolite have a lower Y/Ni and higher Cr/V ratio. In contrast, felsic rocks such as granite tend to a higher Y/Ni and lower Cr/V ratio (McLennan et al., 1993). Samples from the Badain Jaran Desert display higher Cr/V and lower Y/Ni values than do samples from the red sand dune field, suggesting source regions of the Badain Jaran Desert have relatively more ultramafic detritus than the red sand dune field, although they are all close to the end member of granite and thus the amount of ultramafic fraction does not exceed 5% (Amorosi et al., 2002). The north Qilian orogenic belt was a part of the Paleo-Tethys Ocean (Wang and Liu, 1976), and the well-known North Qilian ophiolite zone (Wang and Liu, 1976; Huang et al., 1977; Xiao et al., 1978) confirms the role of ultramafic detritus as an indicator of sediment provenance from the Qilian Mountains. However, as shown in Fig. 11a, the four samples B1, B2, B4 and L1 falling closer to range values of red sand dune field are all from Juyan lake and Guaizihu (Figs. 1 and 10) which are more closer to the Altay Mountains and Mongolian Gobi, suggesting an increased source contribution from the Altay Mountains and Mongolian Gobi and thus decreased Cr/V and increased Y/Ni ratios.

5.3. Implication for tracing provenance of loess sediments

Deciphering the ultimate source of desert sands is critical for revealing the source regions of Asian dust deposit and its response to global palaeoclimatic changes (Chen and Li, 2013; Stevens et al., 2013). Loess on CLP is spatially associated with adjacent deserts in north and northwest China, such as Badain Jaran, Tengger and Maowusu deserts. However, their relationship and the role of adjacent deserts in supplying dust to CLP have been the subject of considerable debate (Sun, 2002; Wang et al., 2004; Sun et al., 2007, 2008; Stevens et al., 2010, 2013). Many studies (Yang, 2001; Chen et al., 2007; Sun et al., 2007, 2008; Chen and Li, 2011; Li et al., 2011; Che and Li, 2013) suggested that Alashan Plateau including Badain Jaran, Tengger and Wulanbuhe deserts could be the major source area of the loess on CLP. However, Pullen et al. (2011) challenged this view based on evidence of similar distribution of zircon age spectra between the loess on the CLP and the sediments in Qaidam Basin of the Tibetan Plateau, and proposed that the loess

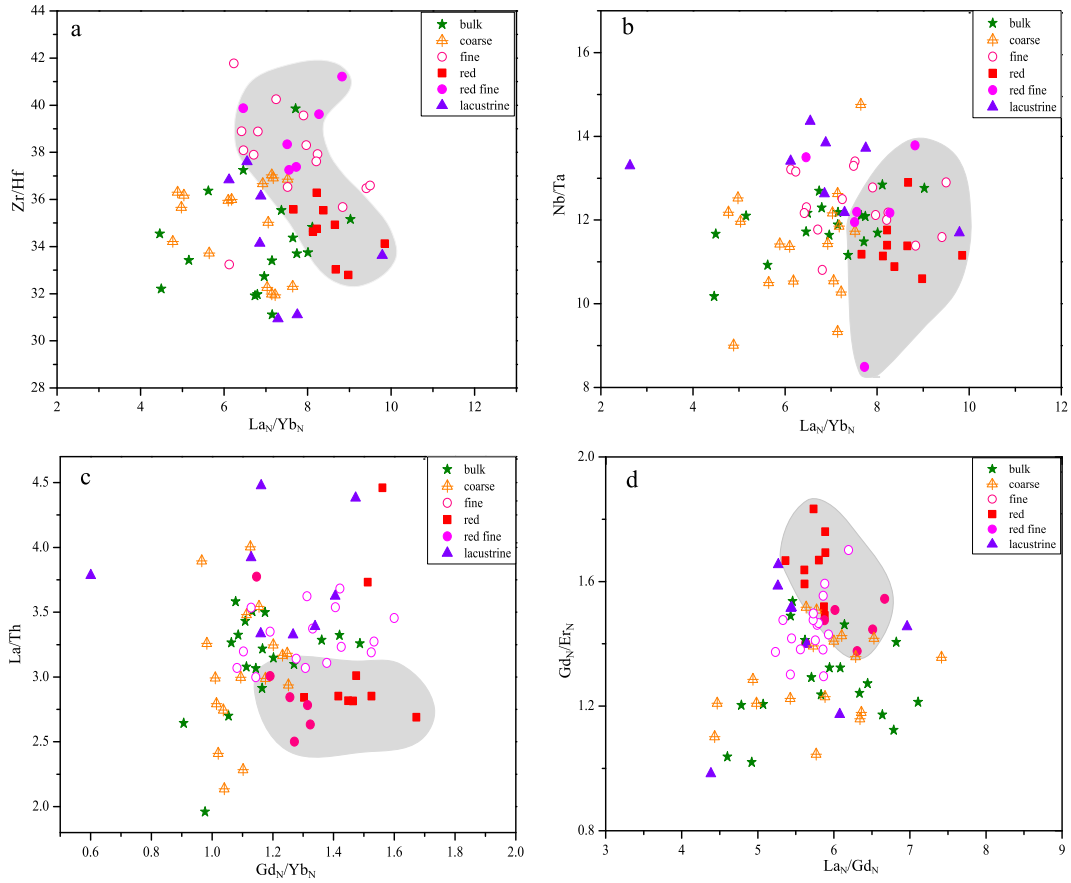

Fig. 9. Bivariate diagrams of trace and rare earth element ratios of samples from the Badain Jaran Desert and the red sand dune field. Keys same as for Fig. 6.

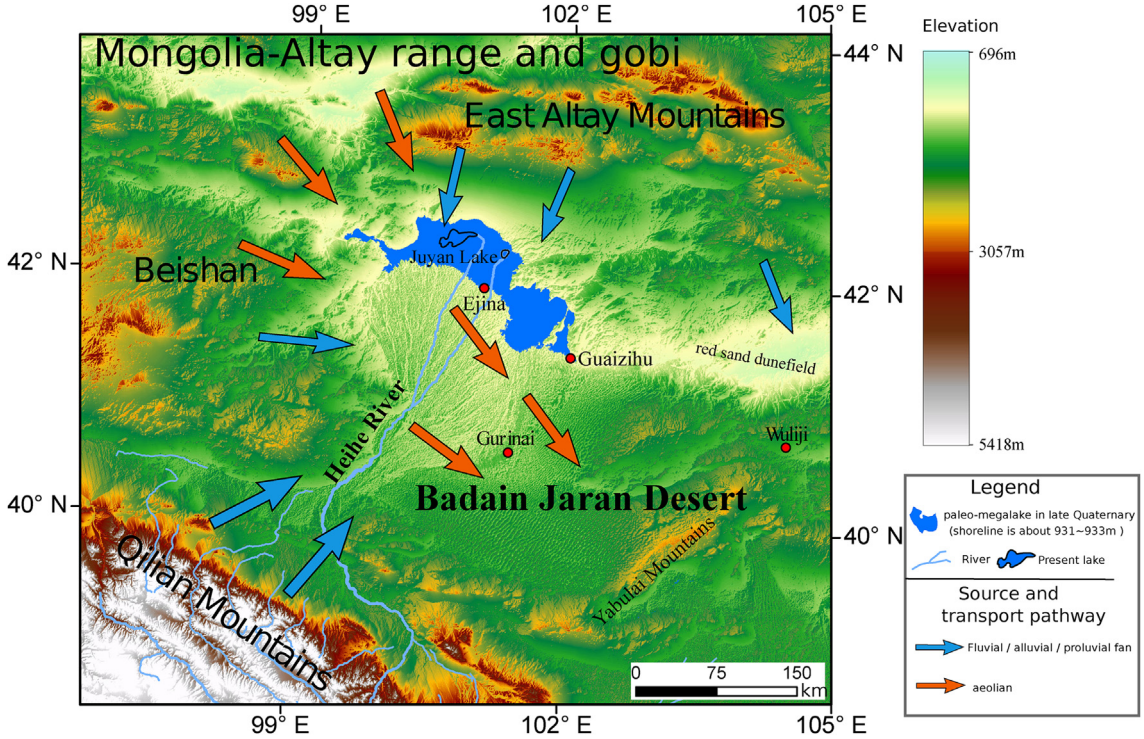

Fig. 10. Schematic graph of source and transport pathways of sands in the Badain Jaran Desert showing source contribution from Qilian Mountains and Gobi Altay Mountains via fluvial-alluvial and aeolian processes. Dried palaeo-megalake (Yang, 1991; Wang et al., 2011) beds are potentially direct sediment sources for aeolian transportation.

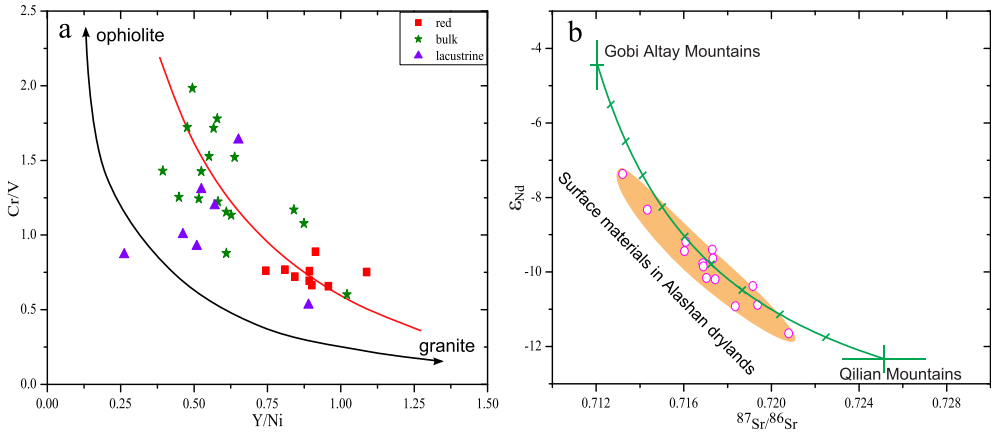

Fig. 11. Binary plots of (a) Y/Ni vs. Cr/V for different samples, mixing line between ophiolite and granite end-members indicating relative proportion of ultramafic and felsic rocks in the source regions. The plot of Y/Ni vs. Cr/V showing source materials from the Qilian Mountains tend to have higher ultramafic components than from Gobi Altay Mountains, and implying a mixture of binary source from Qilian Mountains and Gobi Altay Mountains for the Badain Jaran Desert sands; (b) $^{87}Sr/^{86}Sr$ vs. ε_{Nd} (modified from Li et al., 2011; Chen and Li, 2013), mixing line between Qilian Mountains and Gobi Altay Mountains end-members. Keys same as for Fig. 5.

on the CLP was dominantly sourced from NTP and the Qaidam Basin and transported by westerly winds during glacial times due to equatorward shifting of the subtropical jet streams. Furthermore, based on evidence from zircon ages and heavy mineral assemblages, Stevens et al. (2013) demonstrated that western Maowusu Desert supplied large amount of materials to the CLP via the Yellow River system, and thus there is a genetic link between the Yellow River and associated systems and the formation of the loess deposits.

Although the age spectra of detrital zircon grains is effective in tracing sediment sources (Chen and Li, 2011; Che and Li, 2013; Stevens et al., 2013), it could not identify the transport pathways of sediments. The similarity of the age spectra of detrital zircon between sediments from the CLP and Qaidam Basin and western Maowusu Desert could not prove that loess on CLP is directly sourced from these regions. The zircon grains of loess on CLP with age distributions similar to those of NTP materials could be transported indirectly from the Alashan Plateau via northwest winds. Geomorphologically, Alashan Plateau is a sediment sink for materials from NTP, consistent with geochemical studies based on samples taken from desert margins (Li et al., 2011; Chen and Li, 2011; Che and Li, 2013). Our geomorphological field work and geochemical data comprehensively demonstrate that the sediments in the Badain Jaran Desert have been predominantly derived from the Qilian Mountains of NTP via fluvial processes, implying that zircon grains of the Badain Jaran Desert sands should have similar age distributions to those of NTP, although relevant data are not yet available. Therefore, zircon grains of loess on CLP with age distributions similar to those of NTP materials should not be viewed as convincing evidence against the opinion that loess on CLP could be derived from the Alashan Plateau including the Badain Jaran Desert.

Although a sample collected from the Tengger desert shows a different distribution of zircon age, compared to NTP materials (Stevens et al., 2010), this may be caused by the geographical location of the sampling site. This sample from the Tengger Desert (38°35′20.94″N, 105°28′40.22″E) is very close to the west piedmont of the Helan Mountains. Thus, this single sample should be considered to be a signal of Helan Mountains' materials. Although silt grains comprising most of the loess are scare in dune sands, dust-sized quartz particles can be produced in deserts by a variety of processes including particle impact and salt weathering (Goudie et al., 1979; Cooke et al., 1993; Smith et al., 2002; Crouvi et al., 2010, 2012).

6. Conclusions

Data of major and trace elements show that element concentrations vary considerably in the sediments of the Badain Jaran Desert with regard to sampling locations and grain size fractions. This kind of variation reflects changes of regional lithologies and the effect of particle size. In contrast, aeolian sands in the small dune field of red sands in the northeast are rather homogeneous, suggesting a single source. The trace elements and REE ratios show a distinct discrimination between samples from the Badain Jaran Desert and the red sand dune field although all are characterized by steep light-REE (LREE) and relatively flat heavy-REE (HREE) patterns. Only a few samples' fine fractions from the Badain Jaran Desert resemble the samples from the red sand dune field in some plots of trace elements and REE ratios. Aeolian sands in the Badain Jaran Desert are characterized with negative Ce anomalies and with similar REE ratios with the lacustrine sediments in the region, indicating their direct sources presumably from fluvial, lake and marsh environments, consistent with the occurrence of extensive dry lake beds in the west and northwest of the desert. Source discrimination diagrams of A–CN–K, La–Th–Sc and Zr/Co vs. Th/Co, together with the Al_2O_3/TiO_2 and Zr/Hf ratios suggest both aeolian and lacustrine sediments in the Badain Jaran Desert should be mainly derived from mixed source rocks of granite, granitoids and granodiorite, although some samples' fine fractions show features of strong sedimentary recycling. By comparing immobile trace elements and REE ratios of samples from the Badain Jaran Desert, red sand dune field to the rocks in their potential sand source areas, we conclude that the aeolian sediments in the Badain Jaran Desert have a mixture of binary provenances, with one derived from Qilian Mountains via the drainage system of the Heihe River, and another from the Altay Mountains and Mongolian Gobi via deflation of northwest winds and alluvial processes. The Qilian Mountains of NTP contribute a significant volume of sediments to the Badain Jaran Desert and the Alashan drylands overall, implying that the zircon grains of loess on CLP with age distributions similar to those of NTP materials could still be derived directly from the Badain Jaran Desert by northwest winds.

Acknowledgments

This study has been supported by the National Natural Science Foundation of China (Grant nos.: 41172325; 41430532) and the CAS Strategic Priority Research Program (grant no.: XDA05120502).

Sincere thanks are extended to Prof. Martin Williams, anonymous reviewers and Editor-in-Chief Prof. Colin V. Murray-Wallace for their very valuable comments and suggestions.

Appendix A. Supplementary data

Supplementary data related to this article can be found at http://dx.doi.org/10.1016/j.quascirev.2015.10.039.

References

Ahmad, I., Chandra, R., 2013. Geochemistry of loess-paleosol sediments of Kashmir Valley, India: provenance and weathering. J. Asian Earth Sci. 66, 73–89.

Amorosi, A., Centineo, M.C., Dinelli, E., Lucchini, F., Tateo, F., 2002. Geochemical and mineralogical variations as indicators of provenance changes in Late Quaternary deposits of SE Po Plain. Sediment. Geol. 151, 273–292.

Arimoto, R., 2001. Eolian dust and climate: relationships to sources, tropospheric chemistry, transport and deposition. Earth Sci. Rev. 54, 29–42.

Bahlburg, H., Dobrzinski, N., 2011. A review of the Chemical Index of Alteration (CIA) and its application to the study of Neoproterozoic glacial deposits and climate transitions. Geol. Soc. Lond. Mem. 36, 81–92.

Batchelor, R.A., Bowden, P., 1985. Petrogenetic interpretation of granitoid rock series using multicationic parameters. Chem. Geol. 48, 43–55.

Cai, H., 1986. Discussion of Quaternary stratigraphic division in the Badain Jaran desert. Acta Geol. Gansu 3, 142–152 (in Chinese).

Castillo, S., Moreno, T., Querol, X., Alastuey, A., Cuevas, E., Herrmann, L., Mounkaila, M., Gibbons, W., 2008. Trace element variation in size-fractionated African desert dusts. J. Arid Environ. 72, 1034–1045.

Chase, B., 2009. Evaluating the use of dune sediments as a proxy for palaeo-aridity: a southern African case study. Earth Sci. Rev. 93, 31–45.

Chase, B.M., Thomas, D.S.G., 2006. Late Quaternary dune accumulation along the western margin of South Africa: distinguishing forcing mechanisms through the analysis of migratory dune forms. Earth Planet. Sci. Lett. 251, 318–333.

Chase, B.M., Brewer, S., 2009. Last Glacial Maximum dune activity in the Kalahari Desert of southern Africa: observations and simulations. Quat. Sci. Rev. 28, 301–307.

Che, X., Li, G., 2013. Binary sources of loess on the Chinese Loess Plateau revealed by U–Pb ages of zircon. Quat. Res. 80, 545–551.

Chen, J., Li, G.J., Yang, J.D., Rao, W.B., Lu, H.Y., Balsam, W., Sun, Y.B., Ji, J.F., 2007. Nd and Sr isotopic characteristics of Chinese deserts: implications for the provenances of Asian dust. Geochim. Cosmochim. Acta 71, 3904–3914.

Chen, J., Li, G., 2011. Geochemical studies on the source region of Asian dust. Sci. China Earth Sci. 54, 1279–1301.

Chen, Z., Li, G., 2013. Evolving sources of eolian detritus on the Chinese Loess Plateau since early Miocene: tectonic and climatic controls. Earth Planet. Sci. Lett. 371, 220–225.

Condie, K.C., Dengate, J., Cullers, R.L., 1995. Behavior of rare earth elements in a paleoweathering profile on granodiorite in the Front Range, Colorado, USA. Geochim. Cosmochim. Acta 59, 279–294.

Cooke, R., Warren, A., Goudie, A., 1993. Desert Geomorphology. UCL Press, London.

Cox, R., Lowe, D.R., Cullers, R.L., 1995. The influence of sediment recycling and basement composition on evolution of mudrock chemistry in the southwestern United States. Geochim. Cosmochim. Acta 59, 2919–2940.

Cohen, T.J., Nanson, G.C., Larsen, J.R., Jones, B.G., Price, D.M., Coleman, M., Pietsch, T.J., 2010. Late Quaternary aeolian and fluvial interactions on the Cooper Creek Fan and the association between linear and source-bordering dunes, Strzelecki Desert, Australia. Quat. Sci. Rev. 29, 455–471.

Crouvi, O., Amit, R., Enzel, Y., Gillespie, A.R., 2010. Active sand seas and the formation of desert loess. Quat. Sci. Rev. 29, 2087–2098.

Crouvi, O., Schepanski, K., Amit, R., Gillespie, A.R., Enzel, Y., 2012. Multiple dust sources in the Sahara Desert: the importance of sand dunes. Geophys. Res. Lett. 39, L13401.

Cullers, R.L., Podkovyrov, V.N., 2002. The source and origin of terrigenous sedimentary rocks in the Mesoproterozoic Ui group, southeastern Russia. Precambrian Res. 117, 157–183.

Cunningham, D., 2013. Mountain building processes in intracontinental oblique deformation belts: lessons from the Gobi Corridor, Central Asia. J. Struct. Geol. 46, 255–282.

Dong, Z., Qian, G., Lv, P., Hu, G., 2013. Investigation of the sand sea with the tallest dunes on Earth: China's Badain Jaran Sand Sea. Earth Sci. Rev. 120, 20–39.

Economos, R.C., Hanzl, P., Hrdlickova, K., Burianek, D., Said, L., Gerdes, A., Paterson, S.R., 2008. Geochemical and structural constraints on the magmatic history of the Chandman Massif of the eastern Mongolian Altay Range, SW Mongolia. J. Geosci. 53, 335–352.

Fedo, C.M., Nesbitt, H.W., Young, G.M., 1995. Unraveling the effects of potassium metasomatism in sedimentary rocks and paleosols, with implications for paleoweathering conditions and provenance. Geology 23, 921–924.

Ferrat, M., Weiss, D.J., Strekopytov, S., Dong, S., Chen, H., Najorka, J., Sun, Y., Gupta, S., Tada, R., Sinha, R., 2011. Improved provenance tracing of Asian dust sources using rare earth elements and selected trace elements for palaeomonsoon studies on the eastern Tibetan Plateau. Geochim. Cosmochim. Acta 75, 6374–6399.

Fryberger, S., Dean, G., 1979. Dune forms and wind regime. In: McKee, E. (Ed.), A Study of Global Sand Seas: United States Geological Survey Professional Paper, 1052, Washington, pp. 137–169.

Gao, Q., Tao, Z., Li, B., Jin, H., Zou, X., Zhang, Y., Dong, G., 2006. Palaeomonsoon variability in the southern fringe of the Badain Jaran Desert, China, since 130 ka BP. Earth Surf. Process. Landf. 31, 265–283.

Garcia, D., Fonteilles, M., Moutte, J., 1994. Sedimentary fractionations between Al, Ti, and Zr and the genesis of strongly peraluminous granites. J. Geol. 102, 411–422.

Girty, G.H., Ridge, D.L., Knaack, C., Johnson, D., Al-Riyami, R.K., 1996. Provenance and depositional setting of Paleozoic chert and argillite, Sierra Nevada, California. J. Sediment. Res. 66, 107–118.

Goudie, A., 2009. Dust storms: recent developments. J. Environ. Manag. 90, 89–94.

Goudie, A., Cooke, R., Doornkamp, J., 1979. The formation of silt from quartz dune sand by salt weathering in deserts. J. Arid Environ. 2, 105–112.

Guo, Y., Li, B., Wen, X., Wang, F., Niu, D., Shi, Y., Guo, Y., Jiang, S., Hu, G., 2014. Holocene climate variation determined from rubidium and strontium contents and ratios of sediments collected from the BadainJaran Desert, Inner Mongolia, China. Chem. Erde Geochem. 74, 571–576.

Hanzl, P., Bat-Ulzii, D., Rejchrt, M., Kosler, J., Bolormaa, K., Hrdlickova, K., 2008. Geology and geochemistry of the Palaeozoic plutonic bodies of the Trans-Altay Gobi, SW Mongolia: implications for magmatic processes in an accreted volcanic-arc system. J. Geosci. 53, 201–234.

Hara, Y., Uno, I., Wang, Z., 2006. Long-term variation of Asian dust and related climate factors. Atmos. Environ. 40, 6730–6740.

Harris, N.B.W., Ronghua, X., Lewis, C.L., Hawkesworth, C.J., Yuquan, Z., 1988. Isotope geochemistry of the 1985 Tibet Geotraverse, Lhasa to Golmud. Philos. Trans. R. Soc. Lond. Math. Phys. Eng. Sci. 327, 263–285.

Heller, F., Liu, T., 1984. Magnetism of Chinese loess deposits. Geophys. J. Int. 77, 125–141.

Honda, M., Yabuki, S., Shimizu, H., 2004. Geochemical and isotopic studies of aeolian sediments in China. Sedimentology 51, 211–230.

Huang, H., Niu, Y., Nowell, G., Zhao, Z., Yu, X., Zhu, D., Mo, X., Ding, S., 2014. Geochemical constraints on the petrogenesis of granitoids in the East Kunlun Orogenic belt, northern Tibetan Plateau: implications for continental crust growth through syn-collisional felsic magmatism. Chem. Geol. 370, 1–18.

Huang, J., Ren, J., Jiang, C., Zhang, Z., Xu, Z., 1977. An outline of the tectonic characteristics of China. Acta Geol. Sin. 51, 117–135 (in Chinese with English abstract).

Jolivet, M., Ritz, J., Vassallo, R., Larroque, C., Braucher, R., Todbileg, M., Chauvet, A., Sue, C., Arnaud, N., De Vicente, R., 2007. Mongolian summits: an uplifted, flat, old but still preserved erosion surface. Geology 35, 871–874.

Kasper Zubillaga, J.J., Zolezzi Ruíz, H., Carranza Edwards, A., Girón García, P., Ortiz Zamora, G., Palma, M., 2007. Sedimentological, modal analysis and geochemical studies of desert and coastal dunes, Altar Desert, NW Mexico. Earth Surf. Process. Landf. 32, 489–508.

Lancaster, N., 2008. Desert dune dynamics and development: insights from luminescence dating. Boreas 37, 559–573.

Lancaster, N., Baker, S., Bacon, S., McCarley-Holder, G., 2015. Owens Lake dune fields: composition, sources of sand, and transport pathways. Catena 134, 41–49.

Li, G., Pettke, T., Chen, J., 2011. Increasing Nd isotopic ratio of Asian dust indicates progressive uplift of the north Tibetan Plateau since the middle Miocene. Geology 39, 199–202.

López, J.M.G., Bauluz, B., Fernández-Nieto, C., Oliete, A.Y., 2005. Factors controlling the trace-element distribution in fine-grained rocks: the Albian kaolinite-rich deposits of the Oliete Basin (NE Spain). Chem. Geol. 214, 1–19.

Lou, T., 1962. The formation and utilization of the desert between Minqing and Badain Monastery. Res. Desert Control 3, 90–95 (in Chinese).

Maher, B.A., Prospero, J.M., Mackie, D., Gaiero, D., Hesse, P.P., Balkanski, Y., 2010. Global connections between aeolian dust, climate and ocean biogeochemistry at the present day and at the last glacial maximum. Earth Sci. Rev. 99, 61–97.

Mason, J.A., Lu, H., Zhou, Y., Miao, X., Swinehart, J.B., Liu, Z., Goble, R.J., Yi, S., 2009. Dune mobility and aridity at the desert margin of northern China at a time of peak monsoon strength. Geology 37, 947–950.

McLennan, S.M., 1989. Rare earth elements in sedimentary rocks; influence of provenance and sedimentary processes. Rev. Miner. Geochem. 21, 169–200.

McLennan, S.M., Hemming, S., McDaniel, D.K., Hanson, G.N., 1993. Geochemical approaches to sedimentation, provenance, and tectonics. Geol. Soc. Am. Special Pap. 284, 21–40.

Mischke, S., 2005. New evidence for origin of Badain Jaran Desert of Inner Mongoliafrom granulometry and thermoluminescence dating. J. Palaeogeogr. 7, 79–97.

Molnar, P., 2004. Late cenozoic increase in accumulation rates of terrestrial sediment: how might climate change have affected erosion rates? Annu. Rev. Earth Planet. Sci. 32, 67–89.

Moreno, T., Querol, X., Castillo, S., Alastuey, A., Cuevas, E., Herrmann, L., Mounkaila, M., Elvira, J., Gibbons, W., 2006. Geochemical variations in aeolian mineral particles from the Sahara-Sahel Dust Corridor. Chemosphere 65, 261–270.

Muhs, D.R., Stafford, T.W., Cowherd, S.D., Mahan, S.A., Kihl, R., Maat, P.B., Bush, C.A., Nehring, J., 1996. Origin of the late Quaternary dune fields of northeastern Colorado. Geomorphology 17, 129–149.

Muhs, D.R., Reynolds, R.L., Been, J., Skipp, G., 2003. Eolian sand transport pathways in the southwestern United States: importance of the Colorado River and local

sources. Quat. Int. 104, 3–18.
Muhs, D.R., Roskin, J., Tsoar, H., Skipp, G., Budahn, J.R., Sneh, A., Porat, N., Stanley, J., Katra, I., Blumberg, D.G., 2013. Origin of the Sinai-Negev erg, Egypt and Israel: mineralogical and geochemical evidence for the importance of the Nile and sea level history. Quat. Sci. Rev. 69, 28–48.
Murray, R.W., 1994. Chemical criteria to identify the depositional environment of chert: general principles and applications. Sediment. Geol. 90, 213–232.
Munyikwa, K., 2005. The role of dune morphogenetic history in the interpretation of linear dune luminescence chronologies: a review of linear dune dynamics. Prog. Phys. Geogr. 29, 317–336.
Nesbitt, H.W., Young, G.M., 1982. Early Proterozoic climates and plate motions inferred from major element chemistry of lutites. Nature 299, 715–717.
Nesbitt, H.W., Markovics, G., 1997. Weathering of granodioritic crust, long-term storage of elements in weathering profiles, and petrogenesis of siliciclastic sediments. Geochim. Cosmochim. Acta 61, 1653–1670.
Preusser, F., Radies, D., Matter, A., 2002. A 160,000-year record of dune development and atmospheric circulation in Southern Arabia. Science 296, 2018–2020.
Pullen, A., Kapp, P., McCallister, A.T., Chang, H., Gehrels, G.E., Garzione, C.N., Heermance, R.V., Ding, L., 2011. Qaidam Basin and northern Tibetan Plateau as dust sources for the Chinese Loess Plateau and paleoclimatic implications. Geology 39, 1031–1034.
Scheuvens, D., Schütz, L., Kandler, K., Ebert, M., Weinbruch, S., 2013. Bulk composition of northern African dust and its source sediments-a compilation. Earth Sci. Rev. 116, 170–194.
Singhvi, A.K., Porat, N., 2008. Impact of luminescence dating on geomorphological and palaeoclimate research in drylands. Boreas 37, 536–558.
Skonieczny, C., Bory, A., Bout-Roumazeilles, V., Abouchami, W., Galer, S.J.G., Crosta, X., Stuut, J.B., Meyer, I., Chiapello, I., Podvin, T., Chatenet, B., Diallo, A., Ndiaye, T., 2011. The 7–13 March 2006 major Saharan outbreak: multiproxy characterization of mineral dust deposited on the West African margin. J. Geophys. Res. Atmos. 116, D18210.
Smith, B., Wright, J., Whalley, W., 2002. Sources of non-glacial, loesssize quartz silt and the origins of "desert loess". Earth Sci. Rev. 59, 1–26.
Stevens, T., Palk, C., Carter, A., Lu, H., Clift, P.D., 2010. Assessing the provenance of loess and desert sediments in northern China using U–Pb dating and morphology of detrital zircons. Geol. Soc. Am. Bull. 122, 1331–1344.
Stevens, T., Carter, A., Watson, T.P., Vermeesch, P., Andò, S., Bird, A.F., Lu, H., Garzanti, E., Cottam, M.A., Sevastjanova, I., 2013. Genetic linkage between the Yellow River, the Mu Us desert and the Chinese Loess Plateau. Quat. Sci. Rev. 78, 358–368.
Sun, P., Sun, D., 1964. The hydrological geology of the western Inner Mongolia. Res. Desert Control 6, 245–317 (in Chinese).
Sun, J., 2002. Provenance of loess material and formation of loess deposits on the Chinese Loess Plateau. Earth Planet. Sci. Lett. 203, 845–859.
Sun, Y., Tada, R., Chen, J., Chen, H., Toyoda, S., Tani, A., Isozaki, Y., Nagashima, K., Hasegawa, H., Ji, J., 2007. Distinguishing the sources of Asian dust based on electron spin resonance signal intensity and crystallinity of quartz. Atmos. Environ. 41, 8537–8548.
Sun, Y.B., Tada, R.J., Chen, J.C., Liu, Q.S., Toyoda, S., Tani, A., Ji, J.F., Isozaki, Y., 2008. Tracing the provenance of fine-grained dust deposited on the central Chinese Loess Plateau. Geophys. Res. Lett. 35, L01804.
Taylor, S.R., McLennan, S.M., 1985. The Continental Crust: its Composition and Evolution. Blackwell, Oxford.
Thomas, D.S., Wiggs, G.F., 2008. Aeolian system responses to global change: challenges of scale, process and temporal integration. Earth Surf. Process. Landf. 33, 1396–1418.
Thomas, D.S., Burrough, S.L., 2012. Interpreting geoproxies of late Quaternary climate change in African drylands: implications for understanding environmental change and early human behaviour. Quat. Int. 253, 5–17.
Tian, Z., Xiao, W., Windley, B.F., Lin, L., Han, C., Zhang, J., Wan, B., Ao, S., Song, D., Feng, J., 2014. Structure, age, and tectonic development of the Huoshishan–Niujuanzi ophiolitic mélange, Beishan, southernmost Altayds. Gondwana Res. 25, 820–841.
Wan, Y., Zhang, J., Yang, J., Xu, Z., 2006. Geochemistry of high-grade metamorphic rocks of the North Qaidam Mountains and their geological significance. J. Asian Earth Sci. 28, 174–184.
Wang, F., Sun, D., Chen, F., Bloemendal, J., Guo, F., Li, Z., Zhang, Y., Li, B., Wang, X., 2015. Formation and evolution of the Badain Jaran Desert, North China, as revealed by a drill core from the desert centre and by geological survey. Palaeogeogr. Palaeoclimatol. Palaeoecol. 426, 139–158.
Wang, N., Li, Z., Cheng, H., Li, Y., Huang, Y., 2011. High lake levels on Alashan Plateau during the Late Quaternary. Chin. Sci. Bull. 56, 1799–1808.
Wang, Q., Liu, X., 1976. Paleo-oceanic crust of the Chilienshan region, western China and its tectonic significance. Sci. Geol. Sin. 1, 42–55 (in Chinese with English abstract).
Wang, X., Dong, Z., Zhang, J., Liu, L., 2004. Modern dust storms in China: an overview. J. Arid Environ. 58, 559–574.
Williams, M., 2014. Climate Change in Deserts. Cambridge University Press, Cambridge.
Williams, M., 2015. Interactions between fluvial and eolian geomorphic systems and processes: examples from the Sahara and Australia. Catena 134, 4–13.
Windley, B.F., Alexeiev, D., Xiao, W., Kröner, A., Badarch, G., 2007. Tectonic models for accretion of the Central Asian Orogenic Belt. J. Geol. Soc. 164, 31–47.
Wünnemann, B., Hartmann, K., Altmann, N., Hambach, U., Pachur, H., Zhang, H., 2007. Interglacial and glacial fingerprints from lake deposits in the Gobi Desert, NW China. Dev. Quat. Sci. 7, 323–347.
Xiao, X., Chen, G., Zhu, Z., 1978. A preliminary study on the tectonics of ancient ophiolites in the Qilian Mountain, Northwest China. Acta Geol. Sin. 54, 281–295 (in Chinese with English abstract).
Yan, M., Wang, G., Li, B., Dong, G., 2001. Formation and growth of high mega-dunes in Badain Jaran Desert. Acta Geogr. Sin. 56, 83–91 (in Chinese with English abstract).
Yan, Z., Xiao, W.J., Windley, B.F., Wang, Z.Q., Li, J.L., 2010. Silurian clastic sediments in the North Qilian Shan, NW China: chemical and isotopic constraints on their forearc provenance with implications for the Paleozoic evolution of the Tibetan Plateau. Sediment. Geol. 231, 98–114.
Yang, X., 1991. Geomorphologische Untersuchungen in Trockenräumen NW-Chinas unter besonderer Berücksichtigung von Badanjilin und Takelamagan. Göttinger Geogr. Abh. 96, 1–124.
Yang, X., 2001. Late Quaternary evolution and paleoclimates, western Alashan Plateau, Inner Mongolia, China. Z. für Geomorphol. N. F. 45, 1–16.
Yang, X., Goudie, A., 2007. Geomorphic processes and palaeoclimatology in deserts. Quat. Int. 175, 1–2.
Yang, X., Liu, T., Xiao, H., 2003. Evolution of megadunes and lakes in the Badain Jaran Desert, Inner Mongolia, China during the last 31,000 years. Quat. Int. 104, 99–112.
Yang, X., Liu, Y., Li, C., Song, Y., Zhu, H., Jin, X., 2007. Rare earth elements of aeolian deposits in Northern China and their implications for determining the provenance of dust storms in Beijing. Geomorphology 87, 365–377.
Yang, X., Zhu, B., White, P.D., 2007a. Provenance of aeolian sediment in the Taklamakan Desert of western China, inferred from REE and major-elemental data. Quat. Int. 175, 71–85.
Yang, X., Ma, N., Dong, J., Zhu, B., Xu, B., Ma, Z., Liu, J., 2010. Recharge to the interdune lakes and Holocene climatic changes in the Badain Jaran Desert, western China. Quat. Res. 73, 10–19.
Yang, X., Scuderi, L., Paillou, P., Liu, Z., Li, H., Ren, X., 2011. Quaternary environmental changes in the drylands of China-A critical review. Quat. Sci. Rev. 30, 3219–3233.
Yang, X., Scuderi, L., Liu, T., Paillou, P., Li, H., Dong, J., Zhu, B., Jiang, W., Jochems, A., Weissmann, G., 2011a. Formation of the highest sand dunes on Earth. Geomorphology 135, 108–116.
Yang, X., Wang, X., Liu, Z., Li, H., Ren, X., Zhang, D., Ma, Z., Rioual, P., Jin, X., Scuderi, L., 2013. Initiation and variation of the dune fields in semi-arid China-with a special reference to the Hunshandake Sandy Land, Inner Mongolia. Quat. Sci. Rev. 78, 369–380.
Yang, X., Scuderi, L.A., Wang, X., Scuderi, L.J., Zhang, D., Li, H., Forman, S., Xu, Q., Wang, R., Huang, W., 2015. Groundwater sapping as the cause of irreversible desertification of Hunshandake Sandy Lands, Inner Mongolia, northern China. PNAS 112, 702–706.
Zhang, H., Lu, H., Yi, S., Xu, Z., Zhou, Y., Tan, H., 2013a. Zircon typological analyses of the major deserts/sand fields in northern china and its implication for identifying sediment source. Quat. Res. 33, 334–344 (in Chinese with English abstract).
Zhang, W., Wu, T., Feng, J., Zheng, R., He, Y., 2013b. Time constraints for the closing of the Paleo-Asian Ocean in the Northern Alashan Region: evidence from Wuliji granites. Sci. China Earth Sci. 56, 153–164.